

Hund's metal physics: from SrNiO₂ to NdNiO₂

Y. Wang,¹ C.-J. Kang,² H. Miao,³ and G. Kotliar^{1,2}

¹*Department of Condensed Matter Physics and Materials Science,
Brookhaven National Laboratory, Upton, New York 11973, USA*

²*Department of Physics and Astronomy, Rutgers University, Piscataway, New Jersey 08856, USA*

³*Material Science and Technology Division, Oak Ridge National Laboratory, Oak Ridge, Tennessee 37830, USA*
(Dated: June 30, 2020)

We study the normal state electronic structure of the recently discovered infinite-layer nickelate superconductor, Nd_{1-x}Sr_xNiO₂. Using SrNiO₂ as a reference, we find that Nd_{1-x}Sr_xNiO₂ is a multi-orbital electronic system with characteristic Hund's metal behaviors, such as metallicity, the importance of high-spin configurations, tendency towards orbital differentiation, and the absence of magnetism in regimes which are ordered according to static mean-field theories. In addition, our DFT+DMFT calculations with exact double counting scheme show that despite large charge carrier doping from SrNiO₂ to LaNiO₂, the Ni-3d total occupancy is barely changed due to the decreased hybridization with the occupied oxygen-2p states, and increased hybridization with the unoccupied La-5d states. Our results are in good agreement with the existing resonant inelastic x-ray scattering measurements and pave the way to understand the pairing mechanism of Nd_{1-x}Sr_xNiO₂.

Introduction—Understanding high temperature (high- T_c) superconductors is an outstanding question in the area of quantum materials and presents major unsolved questions. With the discovery of new materials, multiple questions arise: what are the origins of the high- T_c superconductivity and what are the competing orders. Understanding of these questions requires a proper description of the low-energy electronic structure and the correlations presented in the normal state. The recent discovery of superconductivity in the infinite-layer nickelates, Nd_{1-x}Sr_xNiO₂, by Hwang's group [1] raises these questions in a novel context [2].

We have by now, at least four broad classes of unconventional superconducting materials, which have well established phenomenologies: (1) the quasi-one dimensional organics [3]; (2) materials proximate to a Mott-Hubbard or a charge-transfer insulator [4] such as the quasi-two dimensional organic salts [5] and the copper oxide based materials [6–8] which can be described, at low energies, in terms of an effective single band system; (3) intermetallics including rare-earth or actinides heavy-fermion systems [9]; and (4) the more recently discovered iron pnictides and chalcogenides [10, 11]. Numerous efforts have been made to synthesize 3d⁹ nickelate materials that can serve as analogs of the doped copper oxide superconductors, such as La₄Ni₃O₈ [12, 13].

Early on, LaNiO₂ was suggested theoretically to be a cuprate analog by Anisimov *et al.* [14]. However, Lee and Pickett [15] showed that the electronic structure of LaNiO₂, differs significantly from the cuprates, as rare-earth 5d bands were shown to cross the Fermi level as well. Other differences include smaller c -axis and more three-dimensional nature, smaller crystal field splitting and much smaller hybridization strength between the Ni-3d and oxygen-2p states [16]. Alternatively, analogies with heavy-fermion materials have also been proposed [17]. Despite extensive investiga-

tions by experiments [18–26], density functional theory (DFT) [16, 27–36], DFT plus dynamical mean-field theory (DFT+DMFT) [37–39] methods [40–48] and theoretical models [17, 49–54], the nature of the electronic correlations in Nd_{1-x}Sr_xNiO₂ still remains an open question. In particular, a quantitative agreement between experiment and theory is still absent.

In this work, we carry out various electronic structure calculations and analyze the available data for the infinite-layer nickelates at the two ends of hole-doping (LaNiO₂ and SrNiO₂, respectively) as well as the intermediate doping regime. We point out multiple similarities between (La,Sr)NiO₂ and the Hund's metal iron-based superconductors [52, 55, 56], once we take into account obvious differences, the former has a valence close to 3d^{8.5} – 3d⁹ and with low-energy e_g orbitals while the later has Fe d^{5.5} – d^{6.5} valence with low-energy t_{2g} orbitals [10, 11, 57].

Methods—We study LaNiO₂ instead of NdNiO₂ to avoid the issue of Nd-4f orbitals [16, 42]. Although SrNiO₂ does not crystallize in the LaNiO₂ structure [58], in this work, for the purpose of comparison, we assume the same crystal structures ($P4/mmm$, see Fig.S1 in [59]) and use the same lattice parameters $a = b = 3.966\text{\AA}$ and $c = 3.376\text{\AA}$ [16, 60] for both materials. We perform fully charge self-consistent DFT+DMFT calculations using the code, EDMFTF, developed by Haule *et al.* [61] based on the Wien2k package [62]. We choose a wide hybridization energy window from -10 eV to 10 eV with respect to the Fermi level to cover the long tails of Ni $d_{3z^2-r^2}$ and $d_{xz/yz}$ orbitals due to their strong hybridizations with La/Sr 5d states and interstitial- s states [43]. All the five Ni-3d orbitals are considered as correlated ones and a local Coulomb interaction Hamiltonian with rotationally invariant form is applied. We choose $U = 5$ eV and Hund's coupling $J_H = 1$ eV, which are reasonable values for this system [44, 50]. The local An-

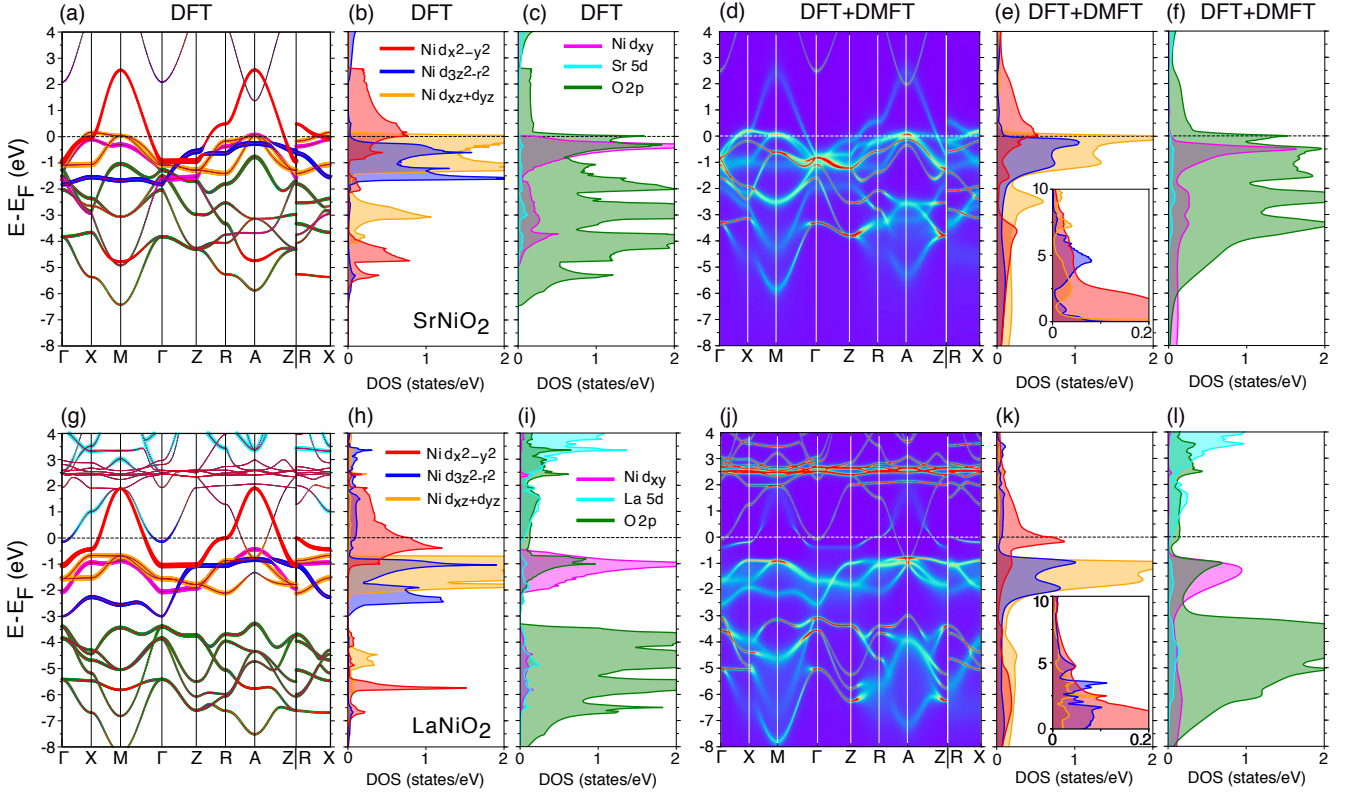


FIG. 1. DFT and DFT+DMFT band structures/ k -resolved spectrum functions and density of states. Upper (lower) panels for SrNiO₂ (LaNiO₂). (a),(g) DFT band structures and (b),(c),(h),(i) DFT density of states. (d),(j) DFT+DMFT k -resolved spectrum functions and (e),(f),(k),(l) DFT+DMFT density of states. The insets in (e) and (k) are the enlarged density of states above the Fermi level from 0 to 10 eV.

person impurity model is solved by the continuous time quantum Monte Carlo (CTQMC) solver [61, 63]. We use an exact double counting (DC) scheme invented by Haule [64], which nearly eliminates the DC issues in most correlated materials. The DFT+DMFT results shown in this work are performed at the temperature $T = 100$ K. The self-energy on real frequency $\Sigma(\omega)$ is obtained by the analytical continuation method of maximum entropy [61]. The local effective mass enhancement due to electronic correlation effects is directly obtained from the self-energy on Matsubara frequency, $m^*/m^{\text{DFT}} = 1/Z = 1 - \frac{\partial \text{Im}\Sigma(i\omega_n)}{\partial \omega_n} \Big|_{\omega_n \rightarrow 0}$, to avoid the large error bar in analytical continuations. The Sr-doping effects are simulated by the virtual crystal approximation (VCA) in the intermediate doping regime ($x \leq 0.5$).

We also perform spin-polarized calculations to check the energetics of long-range magnetic orders on the static mean-field level using the GGA+ U method implemented in the VASP package [65]. A $\sqrt{2} \times \sqrt{2} \times 2$ supercell is used [16, 42]. Four magnetic configurations (see Fig.S2 in [59]) are considered: (i) ferromagnetic (FM), (ii) FM in plane and antiferromagnetic out of plane (AFM-A), (iii) AFM in plane and FM out of plane (AFM-C) and (iv) AFM in plane and AFM out of plane (AFM-G).

Multi-orbital nature and Hund's metal behavior—We start with describing the electronic structure and correlation effects of the material at the extremely hole-doping end, SrNiO₂, as a reference system. Figs. 1(a)-(c) show its DFT band structure and density of states (DOS) that are similar to those of CaCuO₂ [16], but with one electron removed (nominal $3d^8$). It shows an obvious multi-orbital electronic structure with the Fermi level crossing both the e_g and t_{2g} orbitals. The hybridization between Ni- $3d$ and Sr- $5d$ states is very weak. While, the Ni- $3d$ states strongly hybridize with the O- $2p$ states with a sharp peak in the O- $2p$ DOS at the Fermi level [see Fig. 1(c)], such that the charge-transfer energy, Δ_{dp} , between the Ni- $3d$ and O- $2p$ states is small ($2 \sim 3$ eV) [16] compared to Hubbard U , which indicates a possible charge-transfer Mott-insulator scenario like that in NiO [66, 67] if a large Mott gap could be opened. However, our DFT+DMFT calculations show that it is a moderately correlated multi-orbital metal.

Table I show the local occupancy numbers, n_d , and the mass enhancement, m^*/m^{DFT} , of Ni- $3d$ orbitals, and Table II show the probability of the Ni- $3d$ local multiplets, obtained from the DFT+DMFT calculations. The strong $3d$ - $2p$ hybridization leads to a much larger Ni- $3d$ total occupancy (8.479) than the nominal value. Except

for the d_{xy} orbital, all the other $3d$ orbitals are partially occupied and moderately renormalized due to the comparable strengths of Hund's coupling and crystal field splitting. There are 1.057 (0.943), 1.755 (0.245) and 1.845 (0.155) electrons (holes) residing on the $d_{x^2-y^2}$, $d_{3z^2-r^2}$ and $d_{xz/yz}$ orbitals, respectively. These holes are highlighted by the DOS above the Fermi level in the inset of Fig. 1(e). In the presence of large Hund's coupling, they form substantial spin-triplet states ($S = 1$) with a weight of 25.4%, while smaller weight (17.1%) of spin-singlet states in the $N = 8$ sector (see Table II). The Hund's effect is also seen in the DFT+DMFT spectrum functions [see Figs. 1(d) and 1(e)], where the $d_{3z^2-r^2}$ band is pushed closer to the Fermi level compared to the DFT results [Figs. 1(a)]. We find strong charge fluctuations with 7.7%, 43.7% and 5.6% multiplets in the $N = 7, 9$ and 10 sectors, respectively. The electronic correlation strengths exhibit orbital differentiation, with a larger mass enhancement of 1.89 for $d_{x^2-y^2}$ orbital and a smaller one of about 1.6 for $d_{3z^2-r^2}$ and $d_{xz/yz}$ orbitals. Fig. 1(d)-(f) show that all the $3d$ orbitals except d_{xy} contribute to the DFT+DMFT Fermi surfaces (see Fig.S3 in [59]) and that Δ_{dp} is further reduced by the electronic correlation effects.

Thus, SrNiO₂ has many things in common with a correlated multi-orbital metal and manifests Hund's metal behavior [68–74], analogous to iron pnictides and chalcogenides, since it (i) is away from half-filling; (ii) has significant enhancement of electronic correlation and mass; (iii) shows important roles of Hund's coupling and high-spin configurations; (iv) shows orbital differentiation behavior.

We now go to the other end of the undoped LaNiO₂ and examine the evolution of band structures from SrNiO₂ to LaNiO₂ by comparing the DFT band structure and DOS in Figs. 1(g)-(i) to those in Figs. 1(a)-(c). The main changes are (i) the Fermi level moves up; (ii) the Ni $d_{x^2-y^2}$ band is pushed away slightly from the other $3d$ bands; (iii) the La- $5d$ bands start to strongly hybridize with the Ni- $3d$ bands and contribute to the Fermi surfaces [see Γ and A points in Fig. 1(g)]; (iv) the O- $2p$ bands are pushed down a lot to be nearly isolated from the Ni- $3d$ bands and the $3d - 2p$ hybridization becomes much weaker such that Δ_{dp} is significantly reduced. In this work, we also reveal a similar multi-orbital nature of SrNiO₂, even in the undoped LaNiO₂.

Increasing hybridization with La- $5d$ states and decreasing hybridization with O- $2p$ states in LaNiO₂ will lead to electron transfer from the Ni- $3d$ states to La- $5d$ and O- $2p$ states, so the DFT+DMFT calculations give a Ni- $3d$ total occupancy of 8.593 that is greater than SrNiO₂ (8.479) by only 0.11 electrons, even though one more electron is residing in LaNiO₂. This suggests that the Ni- $3d$ total occupancy is almost pinned from the undoped end to the extremely doped end, which has also been confirmed by our doping calculations. The overall change

TABLE I. The local occupancy numbers, n_d , and the mass enhancement, $m^*/m^{\text{DFT}} = 1/Z$, of Ni- $3d$ orbitals from DFT+DMFT calculations.

		$d_{x^2-y^2}$	$d_{3z^2-r^2}$	d_{xz}	d_{yz}	d_{xy}	Total
n_d	SrNiO ₂	1.057	1.755	1.845	1.845	1.977	8.479
	LaNiO ₂	1.219	1.637	1.891	1.891	1.955	8.593
m^*/m^{DFT}	SrNiO ₂	1.89	1.56	1.58	1.58	1.32	
	LaNiO ₂	2.81	1.25	1.21	1.21	1.27	

TABLE II. The weights of the Ni- $3d$ local multiplets sampled by CTQMC solver.

Occupancy N	7	8	8	9	10
Total Spin S	All	1	0	1/2	0
SrNiO ₂ , DMFT	7.7%	25.4%	17.1%	43.7%	5.6%
LaNiO ₂ , DMFT	6.2%	25.9%	10.3%	49.0%	8.1%
LaNiO ₂ , Ref. [18]	6.0%	24.0%	14.0%	56.0%	–

of the Ni- $3d$ total occupancy is only 0.08 in the doping range from $x = 0$ to $x = 0.5$ [see Fig. 3(a)]. Comparing to SrNiO₂, the occupancy numbers among $3d$ orbitals in LaNiO₂ are slightly redistributed, with 0.162 (0.046) more electrons residing on $d_{x^2-y^2}$ ($d_{xz/yz}$) orbitals and 0.118 less electrons residing on $d_{3z^2-r^2}$ orbital, so still with substantial holes residing on these orbitals, as highlighted in the inset of Figs. 1(k). As a result, the probability distribution of the Ni- $3d$ multiplets shown in Table II is not too different between LaNiO₂ and SrNiO₂, so LaNiO₂ also shows multi-orbital nature and strong metallicity. The calculated weight of the spin-triplet configurations is 25.9% for LaNiO₂, which is very close to the value, 24%, given by the multiplet calculation used to simulate the x-ray absorption (XAS) and resonant inelastic x-ray scattering (RIXS) spectra of LaNiO₂ in [18]. Their simulations show that substantial $3d^8$ spin-triplet configurations are responsible for the resonant pre-peak, A' , of RIXS. The critical roles of spin-triplet configurations have also been pointed out in [51]. Different from [40], we obtain a small percentage of the $3d^{10}$ configuration (8.1%) that rules out the possibility of the charge-transfer Mott insulator scenario in LaNiO₂. The percentages of other multiplets obtained here are also very close to the values given by [18], which validates our DFT+DMFT calculations.

Going from SrNiO₂ to LaNiO₂, the orbital differentiation is significantly enhanced, with stronger mass enhancement of 2.81 for $d_{x^2-y^2}$ orbital and weaker mass enhancement of about 1.2~1.3 for the other $3d$ orbitals in LaNiO₂. Fig. 3(b) shows that a tendency of increasing correlation in $d_{x^2-y^2}$ orbital and decreasing correlation in other $3d$ orbitals, as decreasing hole-doping level x , has been captured by our doping calculations. As shown in the DFT+DMFT calculations by Lechermann [47, 48],

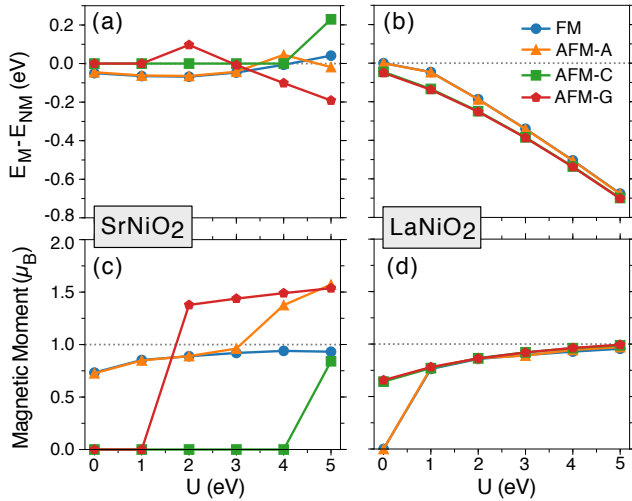


FIG. 2. (a),(b) The total energy difference (per the unit cell containing one Ni site) between the magnetic states and the non-magnetic state, $E_M - E_{NM}$, vs the Hubbard U from the GGA+ U calculations. (c),(d) The ordered magnetic moments per one Ni site vs U . (a),(c) for SrNiO₂ and (b),(d) for LaNiO₂.

a large enough Hubbard U (≥ 10 eV) can open a Mott gap in the $d_{x^2-y^2}$ orbital. Our results strongly support their claim that the multi-orbital nature rules the normal state of NdNiO₂ [47, 48], but with strong metallicity in $d_{x^2-y^2}$ orbital found in our work. Fig. 3(a) shows the evolution of the DFT+DMFT Fermi surface as increasing hole-doping. We find Lifshitz transitions of the Fermi surface from $x = 0$ to $x = 0.5$ and two sheets of Fermi surfaces around the optimal doping level, $x \approx 0.2$. The results of occupancy numbers and mass enhancement of Ni $d_{x^2-y^2}$ and $d_{3z^2-r^2}$ orbitals as well as the evolution of Fermi surfaces as increasing hole-doping presented in this work are consistent with the previous DFT+DMFT study with $U = 6$ eV, $J_H = 0.95$ eV and fully localized DC scheme [44].

Magnetism—One of the main arguments to question the cuprate-like superconducting nature in Nd_{1-x}Sr_xNiO₂ is that the super-exchange coupling J_{ex} is too small due to the very large Δ_{dp} [51]. Here, like CaCuO₂ [16, 40], Δ_{dp} is significantly decreased in SrNiO₂, which may stabilize long-range AFM orders or induce stronger AFM fluctuations through an enhanced J_{ex} . We check this by comparing the ground state energy of possible magnetic configurations in SrNiO₂ to that in LaNiO₂ on the static mean-field (GGA+ U) level. Figs. 2(a) and 2(b) show the energy difference per one Ni site between the magnetic and non-magnetic (NM) states, $\delta E = E_M - E_{NM}$, as functions of Hubbard U . For SrNiO₂, the lowest energy state is FM and AFM-A when $U \leq 3$ eV and AFM-G when $U > 3$ eV. For LaNiO₂, AFM-G is the lowest energy state, even at the GGA level ($U = 0$) [42]. FM, AFM-A and AFM-C

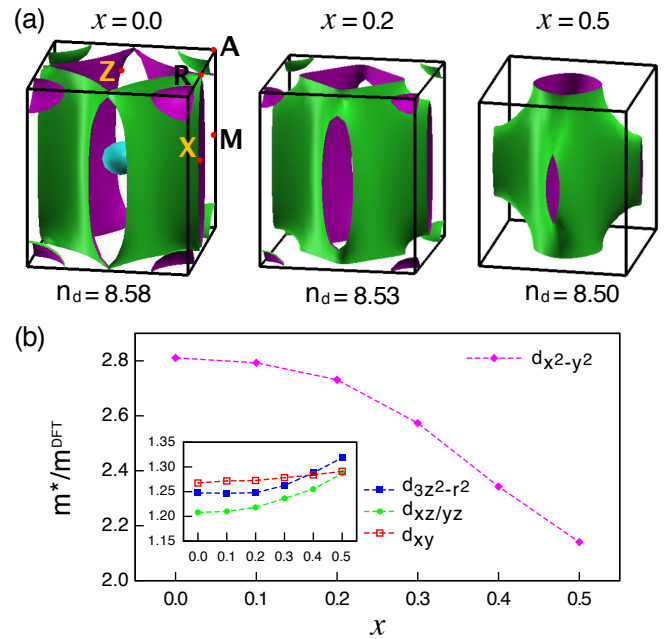


FIG. 3. (a) Evolution of the DFT+DMFT Fermi surfaces and (b) mass enhancement of Ni-3d orbitals as functions of doping level x .

are also lower in energy than the non-magnetic state when $U > 0$. δE of LaNiO₂ becomes much larger than that of SrNiO₂ when $U > 0$, which suggests that it is much easier for LaNiO₂ to stabilize magnetic orders than SrNiO₂, hence the physics of super-exchange is not operational in these materials, while they are essential for the cuprates.

Although the static mean-field calculations can give stable long-range magnetic orders with large ordered magnetic moments [see Figs. 2(c) and 2(d)] in both of LaNiO₂ and SrNiO₂, in reality, no signature of such orders have been observed in LaNiO₂ or NdNiO₂ down to the very low temperature range the available experiments have approached so far [75, 76]. This situation is similar to that in iron-based superconductors, where the static mean-field calculations usually predict stable magnetic orders with large ordered moments while the ordered moments are found to be significantly suppressed in experiments, as discussed widely in literatures such as [71, 77–83].

Conclusion—To summarize, we have provided a new perspective to describe the normal state electronic structure of Nd_{1-x}Sr_xNiO₂ starting using SrNiO₂ as a reference. SrNiO₂ is found to be a moderately correlated multi-orbital Hund-like metal. Going from SrNiO₂ to LaNiO₂, the Ni-3d total occupancy is insensitive to decreasing hole-doping as the changes in carrier density are compensated by decreased hybridization with the occupied O-2p states and increased hybridization with the unoccupied La-5d states. Thus, as in SrNiO₂, same amount

of high-spin configurations, same order of charge fluctuation and similar multi-orbital nature but with enhanced orbital differentiation, are found in LaNiO_2 . Our results are in good agreement with the existing RIXS measurements.

From this perspective, our study excludes the cuprate-like scenario for this new Ni-based superconductor and suggests that $\text{Nd}_{1-x}\text{Sr}_x\text{NiO}_2$ is a new unconventional superconductor that shares many similarities with Hund's superconductors [52, 55, 56], such as their metallicity, the importance of Hund's coupling and high-spin configurations, tendency towards orbital differentiation with the $d_{x^2-y^2}$ as the most correlated orbital, and the absence of magnetism in regimes which are ordered according to static mean-field theories, but with a valence close to $3d^{8.5} - 3d^9$ and with low-energy e_g orbitals instead of the Fe $d^{5.5} - d^{6.5}$ valence with low-energy t_{2g} orbitals [10, 11, 57]. Most interestingly, the ratio between the largest superconducting gap $2\Delta_{max}$ and T_c (determined as the mid-point of the superconducting transition in resistivity) is evaluated to be about 7 from the most recent experimental data of $\text{Nd}_{1-x}\text{Sr}_x\text{NiO}_2$ [84], which is very close to the value for the iron-based superconductors that are proposed as prototypical Hund's superconductors [56, 85].

Finally, we notice that as we place $\text{Nd}_{1-x}\text{Sr}_x\text{NiO}_2$ far from a Mott transition, the insulating behavior observed at low doping and temperatures, has to be attributed to the impurity induced Anderson localization, which should get weaker as sample quality improves.

Note added.—Under the preparation of this manuscript, we learned about the related parameter-free $\text{GW}+\text{EDMFT}$ work [86] that also finds multi-orbital nature and the pinning of the Ni-3d total occupancy in the small doping regime of $\text{Nd}_{1-x}\text{Sr}_x\text{NiO}_2$, which validates our simple $\text{DFT}+\text{DMFT}$ calculations.

Acknowledgment.—We thank Kristjan Haule and Sangkook Choi for very helpful discussions. Y. W., C. K. and G. K. were supported by the U.S. Department of Energy, Office of Science, Basic Energy Sciences as a part of the Computational Materials Science Program through the Center for Computational Design of Functional Strongly Correlated Materials and Theoretical Spectroscopy. H. M. was supported by the Laboratory Directed Research and Development (LDRD) of ORNL, under project No. 10018.

-
- [1] Danfeng Li, Kyuho Lee, Bai Yang Wang, Motoki Osada, Samuel Crossley, Hye Ryoung Lee, Yi Cui, Yasuyuki Hikita, and Harold Y. Hwang, “Superconductivity in an infinite-layer nickelate,” *Nature* **572**, 624–627 (2019).
 [2] Michael R. Norman, “Entering the nickel age of superconductivity,” (2020).
 [3] D. Jérôme, “The physics of organic superconductors,”

- Science* **252**, 1509–1514 (1991).
 [4] J. Zaanen, G. A. Sawatzky, and J. W. Allen, “Band gaps and electronic structure of transition-metal compounds,” *Phys. Rev. Lett.* **55**, 418–421 (1985).
 [5] B. J. Powell and R. H. McKenzie, “Strong electronic correlations in superconducting organic charge transfer salts,” *Journal of Physics: Condensed Matter* **18**, R827–R866 (2006).
 [6] J. G. Bednorz and K. A. Müller, “Possible high- T_c superconductivity in the Ba-La-Cu-O system,” *Zeitschrift für Physik B Condensed Matter* **64**, 189–193 (1986).
 [7] Patrick A. Lee, Naoto Nagaosa, and Xiao-Gang Wen, “Doping a Mott insulator: Physics of high-temperature superconductivity,” *Rev. Mod. Phys.* **78**, 17–85 (2006).
 [8] Elbio Dagotto, “Correlated electrons in high-temperature superconductors,” *Rev. Mod. Phys.* **66**, 763–840 (1994).
 [9] G. R. Stewart, “Heavy-fermion systems,” *Rev. Mod. Phys.* **56**, 755–787 (1984).
 [10] Yoichi Kamihara, Takumi Watanabe, Masahiro Hirano, and Hideo Hosono, “Iron-based layered superconductor $\text{La}[\text{O}_{1-x}\text{F}_x]\text{FeAs}$ ($x=0.05-0.12$) with $T_c = 26$ K,” *Journal of the American Chemical Society* **130**, 3296–3297 (2008).
 [11] G. R. Stewart, “Superconductivity in iron compounds,” *Rev. Mod. Phys.* **83**, 1589–1652 (2011).
 [12] Viktor V. Poltavets, Konstantin A. Lokshin, Andriy H. Nevidomskyy, Mark Croft, Trevor A. Tyson, Joke Hadermann, Gustaaf Van Tendeloo, Takeshi Egami, Gabriel Kotliar, Nicholas ApRoberts-Warren, Adam P. Dioguardi, Nicholas J. Curro, and Martha Greenblatt, “Bulk magnetic order in a two-dimensional $\text{Ni}^{1+}/\text{Ni}^{2+}$ (d^9/d^8) nickelate, isoelectronic with superconducting cuprates,” *Phys. Rev. Lett.* **104**, 206403 (2010).
 [13] Junjie Zhang, D. M. Pajerowski, A. S. Botana, Hong Zheng, L. Harriger, J. Rodriguez-Rivera, J. P. C. Ruff, N. J. Schreiber, B. Wang, Yu-Sheng Chen, W. C. Chen, M. R. Norman, S. Rosenkranz, J. F. Mitchell, and D. Phelan, “Spin stripe order in a square planar trilayer nickelate,” *Phys. Rev. Lett.* **122**, 247201 (2019).
 [14] Vladimir I Anisimov, F Aryasetiawan, and A I Liechtenstein, “First-principles calculations of the electronic structure and spectra of strongly correlated systems: the LDA+U method,” *Journal of Physics: Condensed Matter* **9**, 767–808 (1997).
 [15] K.-W. Lee and W. E. Pickett, “Infinite-layer LaNiO_2 : Ni^{1+} is not Cu^{2+} ,” *Phys. Rev. B* **70**, 165109 (2004).
 [16] A. S. Botana and M. R. Norman, “Similarities and differences between LaNiO_2 and CaCuO_2 and implications for superconductivity,” *Phys. Rev. X* **10**, 011024 (2020).
 [17] Guang-Ming Zhang, Yi-feng Yang, and Fu-Chun Zhang, “Self-doped Mott insulator for parent compounds of nickelate superconductors,” *Phys. Rev. B* **101**, 020501 (2020).
 [18] M. Hepting, D. Li, C. J. Jia, H. Lu, E. Paris, Y. Tseng, X. Feng, M. Osada, E. Been, Y. Hikita, Y.-D. Chuang, Z. Hussain, K. J. Zhou, A. Nag, M. Garcia-Fernandez, M. Rossi, H. Y. Huang, D. J. Huang, Z. X. Shen, T. Schmitt, H. Y. Hwang, B. Moritz, J. Zaanen, T. P. Devereaux, and W. S. Lee, “Electronic structure of the parent compound of superconducting infinite-layer nickelates,” *Nature Materials* **19**, 381–385 (2020).
 [19] Ying Fu, Le Wang, Hu Cheng, Shenghai Pei, Xuefeng Zhou, Jian Chen, Shaoheng Wang, Ran Zhao, Wenrui Jiang, Cai Liu, Mingyuan Huang, Xinwei Wang,

- Yusheng Zhao, Dapeng Yu, Fei Ye, Shanmin Wang, and Jia-Wei Mei, “Core-level x-ray photoemission and Raman spectroscopy studies on electronic structures in Mott-Hubbard type nickelate oxide NdNiO_2 ,” (2019), [arXiv:1911.03177](#).
- [20] Shengwei Zeng, Chi Sin Tang, Xinmao Yin, Changjian Li, Zhen Huang, Junxiong Hu, Wei Liu, Ganesh Ji Omar, Hariom Jani, Zhi Shih Lim, Kun Han, Dongyang Wan, Ping Yang, Andrew T. S. Wee, and Ariando Ariando, “Phase diagram and superconducting dome of infinite-layer $\text{Nd}_{1-x}\text{Sr}_x\text{NiO}_2$ thin films,” (2020), [arXiv:2004.11281](#).
- [21] Danfeng Li, Bai Yang Wang, Kyuho Lee, Shannon P. Harvey, Motoki Osada, Berit H. Goodge, Lena F. Kourkoutis, and Harold Y. Hwang, “Superconducting dome in $\text{Nd}_{1-x}\text{Sr}_x\text{NiO}_2$ infinite layer films,” (2020), [arXiv:2003.08506](#).
- [22] Motoki Osada, Bai Yang Wang, Berit H. Goodge, Kyuho Lee, Hyeok Yoon, Keita Sakuma, Danfeng Li, Masashi Miura, Lena F. Kourkoutis, and Harold Y. Hwang, “A superconducting praseodymium nickelate with infinite layer structure,” *Nano Letters* (2020), [10.1021/acs.nanolett.0c01392](#).
- [23] Berit H. Goodge, Danfeng Li, Motoki Osada, Bai Yang Wang, Kyuho Lee, George A. Sawatzky, Harold Y. Hwang, and Lena F. Kourkoutis, “Doping evolution of the Mott-Hubbard landscape in infinite-layer nickelates,” (2020), [arXiv:2005.02847](#).
- [24] Kyuho Lee, Berit H. Goodge, Danfeng Li, Motoki Osada, Bai Yang Wang, Yi Cui, Lena F. Kourkoutis, and Harold Y. Hwang, “Aspects of the synthesis of thin film superconducting infinite-layer nickelates,” *APL Materials* **8**, 041107 (2020).
- [25] Qing Li, Chengping He, Jin Si, Xiyu Zhu, Yue Zhang, and Hai-Hu Wen, “Absence of superconductivity in bulk $\text{Nd}_{1-x}\text{Sr}_x\text{NiO}_2$,” *Communications Materials* **1**, 16 (2020).
- [26] Bi-Xia Wang, Hong Zheng, E. Kriviyakina, O. Chmaissem, Pietro Papa Lopes, J. W. Lynn, Leighanne C. Gallington, Y. Ren, S. Rosenkranz, J. F. Mitchell, and D. Phelan, “Synthesis and characterization of bulk $\text{Nd}_{1-x}\text{Sr}_x\text{NiO}_2$ and $\text{Nd}_{1-x}\text{Sr}_x\text{NiO}_3$,” (2020), [arXiv:2006.09548](#).
- [27] Peiheng Jiang, Liang Si, Zhaoliang Liao, and Zhicheng Zhong, “Electronic structure of rare-earth infinite-layer $R\text{NiO}_2$ ($R=\text{La}, \text{Nd}$),” *Phys. Rev. B* **100**, 201106 (2019).
- [28] Jiacheng Gao, Zhijun Wang, Chen Fang, and Hongming Weng, “Electronic structures and topological properties in nickelates $\text{Ln}_{n+1}\text{Ni}_n\text{O}_{2n+2}$,” (2019), [arXiv:1909.04657](#).
- [29] Yusuke Nomura, Motoaki Hirayama, Terumasa Tadano, Yoshihide Yoshimoto, Kazuma Nakamura, and Ryotaro Arita, “Formation of a two-dimensional single-component correlated electron system and band engineering in the nickelate superconductor NdNiO_2 ,” *Phys. Rev. B* **100**, 205138 (2019).
- [30] Zhao Liu, Zhi Ren, Wei Zhu, Zhengfei Wang, and Jinlong Yang, “Electronic and magnetic structure of infinite-layer NdNiO_2 : trace of antiferromagnetic metal,” *npj Quantum Materials* **5**, 31 (2020).
- [31] Xianxin Wu, Domenico Di Sante, Tilman Schwemmer, Werner Hanke, Harold Y. Hwang, Srinivas Raghu, and Ronny Thomale, “Robust $d_{x^2-y^2}$ -wave superconductivity of infinite-layer nickelates,” *Phys. Rev. B* **101**, 060504 (2020).
- [32] Mi-Young Choi, Kwan-Woo Lee, and Warren E. Pickett, “Role of $4f$ states in infinite-layer NdNiO_2 ,” *Phys. Rev. B* **101**, 020503 (2020).
- [33] Mi-Young Choi, W. E. Pickett, and K. W. Lee, “Quantum-fluctuation-frustrated flat band instabilities in ndnio_2 ,” (2020), [arXiv:2005.03234](#).
- [34] Motoaki Hirayama, Terumasa Tadano, Yusuke Nomura, and Ryotaro Arita, “Materials design of dynamically stable d^9 layered nickelates,” *Phys. Rev. B* **101**, 075107 (2020).
- [35] Emily Been, Wei-Sheng Lee, Harold Y. Hwang, Yi Cui, Jan Zaanen, Thomas Devereaux, Brian Moritz, and Chunjing Jia, “Theory of Rare-earth Infinite Layer Nickelates,” (2020), [arXiv:2002.12300](#).
- [36] Benjamin Geisler and Rossitza Pentcheva, “Fundamental difference in the electronic reconstruction of infinite-layer vs. perovskite neodymium nickelate films on $\text{SrTiO}_3(001)$,” (2020), [arXiv:2001.03762](#).
- [37] Antoine Georges, Gabriel Kotliar, Werner Krauth, and Marcelo J. Rozenberg, “Dynamical mean-field theory of strongly correlated fermion systems and the limit of infinite dimensions,” *Rev. Mod. Phys.* **68**, 13–125 (1996).
- [38] G. Kotliar, S. Y. Savrasov, K. Haule, V. S. Oudovenko, O. Parcollet, and C. A. Marianetti, “Electronic structure calculations with dynamical mean-field theory,” *Rev. Mod. Phys.* **78**, 865–951 (2006).
- [39] A. I. Lichtenstein, M. I. Katsnelson, and G. Kotliar, “Finite-temperature magnetism of transition metals: An ab initio dynamical mean-field theory,” *Phys. Rev. Lett.* **87**, 067205 (2001).
- [40] Jonathan Karp, Antia S. Botana, Michael R. Norman, Hyowon Park, Manuel Zingl, and Andrew Millis, “Many-body electronic structure of NdNiO_2 and CaCuO_2 ,” *Phys. Rev. X* **10**, 021061 (2020).
- [41] Liang Si, Wen Xiao, Josef Kaufmann, Jan M. Tomczak, Yi Lu, Zhicheng Zhong, and Karsten Held, “Topotactic hydrogen in nickelate superconductors and akin infinite-layer oxides ABO_2 ,” *Phys. Rev. Lett.* **124**, 166402 (2020).
- [42] Siheon Ryeed, Hongkee Yoon, Taek Jung Kim, Min Yong Jeong, and Myung Joon Han, “Induced magnetic two-dimensionality by hole doping in the superconducting infinite-layer nickelate $\text{Nd}_{1-x}\text{Sr}_x\text{NiO}_2$,” *Phys. Rev. B* **101**, 064513 (2020).
- [43] Yuhao Gu, Sichen Zhu, Xiaoxuan Wang, Jiangping Hu, and Hanghui Chen, “A substantial hybridization between correlated Ni- d orbital and itinerant electrons in infinite-layer nickelates,” *Communications Physics* **3**, 84 (2020).
- [44] I. Leonov, S. L. Skornyakov, and S. Y. Savrasov, “Lifshitz transition and frustration of magnetic moments in infinite-layer NdNiO_2 upon hole doping,” *Phys. Rev. B* **101**, 241108 (2020).
- [45] I. Leonov and S. Y. Savrasov, “Effect of epitaxial strain on the electronic structure and magnetic correlations in infinite-layer $(\text{Nd}, \text{Sr})\text{NiO}_2$,” (2020), [arXiv:2006.05295](#).
- [46] Motoharu Kitatani, Liang Si, Oleg Janson, Ryotaro Arita, Zhicheng Zhong, and Karsten Held, “Nickelate superconductors – a renaissance of the one-band Hubbard model,” (2020), [arXiv:2002.12230](#).
- [47] Frank Lechermann, “Late transition metal oxides with infinite-layer structure: nickelates versus cuprates,” *Phys. Rev. B* **101**, 081110 (2020).
- [48] Frank Lechermann, “Multiorbital processes rule the $\text{Nd}_{1-x}\text{Sr}_x\text{NiO}_2$ normal state,” (2020), [arXiv:2005.01166](#).

- [49] Lun-Hui Hu and Congjun Wu, “Two-band model for magnetism and superconductivity in nickelates,” *Phys. Rev. Research* **1**, 032046 (2019).
- [50] Hirofumi Sakakibara, Hidetomo Usui, Katsuhiko Suzuki, Takao Kotani, Hideo Aoki, and Kazuhiko Kuroki, “Model construction and a possibility of cuprate-like pairing in a new d^9 nickelate superconductor (Nd,Sr)NiO₂,” (2019), [arXiv:1909.00060](https://arxiv.org/abs/1909.00060).
- [51] Mi Jiang, Mona Berciu, and George A. Sawatzky, “Critical nature of the Ni spin state in doped NdNiO₂,” *Phys. Rev. Lett.* **124**, 207004 (2020).
- [52] Philipp Werner and Shintaro Hoshino, “Nickelate superconductors: Multiorbital nature and spin freezing,” *Phys. Rev. B* **101**, 041104 (2020).
- [53] Hu Zhang, Lipeng Jin, Shanmin Wang, Bin Xi, Xingqiang Shi, Fei Ye, and Jia-Wei Mei, “Effective Hamiltonian for nickelate oxides Nd_{1-x}Sr_xNiO₂,” *Phys. Rev. Research* **2**, 013214 (2020).
- [54] Ya-Hui Zhang and Ashvin Vishwanath, “Type-II t - j model in superconducting nickelate Nd_{1-x}Sr_xNiO₂,” *Phys. Rev. Research* **2**, 023112 (2020).
- [55] Shintaro Hoshino and Philipp Werner, “Superconductivity from emerging magnetic moments,” *Phys. Rev. Lett.* **115**, 247001 (2015).
- [56] Tsung-Han Lee, Andrey Chubukov, Hu Miao, and Gabriel Kotliar, “Pairing mechanism in Hund’s metal superconductors and the universality of the superconducting gap to critical temperature ratio,” *Phys. Rev. Lett.* **121**, 187003 (2018).
- [57] Qimiao Si, Rong Yu, and Elihu Abrahams, “High-temperature superconductivity in iron pnictides and chalcogenides,” *Nature Reviews Materials* **1**, 16017 (2016).
- [58] H. Pausch and Hk. Mller-Buschbaum, “Prparation von SrNiO₂-einkristallen mit eben koordiniertem Nickel,” *Zeitschrift fr anorganische und allgemeine Chemie* **426**, 184–188 (1976).
- [59] See Supplemental Material at [url] for: the crystal structures, the magnetic configurations and the Fermi surfaces of LaNiO₂ and SrNiO₂. The Supplemental Material includes Refs. [40, 44, 87–90].
- [60] Pierre Levitz, Michel Crespin, and Lucien Gatineau, “Structure of LaNiO₂ by EXAFS and x-ray diffraction: Local environment of Ni⁺¹,” in *EXAFS and Near Edge Structure*, edited by Antonio Bianconi, Lucia Incocchia, and Stanislao Stipcich (Springer Berlin Heidelberg, Berlin, Heidelberg, 1983) pp. 219–221.
- [61] Kristjan Haule, Chuck-Hou Yee, and Kyoo Kim, “Dynamical mean-field theory within the full-potential methods: Electronic structure of CeIrIn₅, CeCoIn₅, and CeRhIn₅,” *Phys. Rev. B* **81**, 195107 (2010).
- [62] Peter Blaha, Karlheinz Schwarz, Fabien Tran, Robert Laskowski, Georg K. H. Madsen, and Laurence D. Marks, “WIEN2k: An APW+lo program for calculating the properties of solids,” *The Journal of Chemical Physics* **152**, 074101 (2020).
- [63] Emanuel Gull, Andrew J. Millis, Alexander I. Lichtenstein, Alexey N. Rubtsov, Matthias Troyer, and Philipp Werner, “Continuous-time monte carlo methods for quantum impurity models,” *Rev. Mod. Phys.* **83**, 349–404 (2011).
- [64] Kristjan Haule, “Exact double counting in combining the dynamical mean field theory and the density functional theory,” *Phys. Rev. Lett.* **115**, 196403 (2015).
- [65] G. Kresse and J. Furthmüller, “Efficient iterative schemes for *ab initio* total-energy calculations using a plane-wave basis set,” *Phys. Rev. B* **54**, 11169–11186 (1996).
- [66] Masatoshi Imada, Atsushi Fujimori, and Yoshinori Tokura, “Metal-insulator transitions,” *Rev. Mod. Phys.* **70**, 1039–1263 (1998).
- [67] T. M. Schuler, D. L. Ederer, S. Itza-Ortiz, G. T. Woods, T. A. Callcott, and J. C. Woicik, “Character of the insulating state in NiO: A mixture of charge-transfer and Mott-Hubbard character,” *Phys. Rev. B* **71**, 115113 (2005).
- [68] Philipp Werner, Emanuel Gull, Matthias Troyer, and Andrew J. Millis, “Spin freezing transition and non-Fermi-liquid self-energy in a three-orbital model,” *Phys. Rev. Lett.* **101**, 166405 (2008).
- [69] K Haule and G Kotliar, “Coherence-incoherence crossover in the normal state of iron oxypnictides and importance of Hund’s rule coupling,” *New Journal of Physics* **11**, 025021 (2009).
- [70] Luca de’ Medici, Jernej Mravlje, and Antoine Georges, “Janus-faced influence of Hund’s rule coupling in strongly correlated materials,” *Phys. Rev. Lett.* **107**, 256401 (2011).
- [71] Z. P. Yin, K. Haule, and G. Kotliar, “Kinetic frustration and the nature of the magnetic and paramagnetic states in iron pnictides and iron chalcogenides,” *Nature Materials* **10**, 932 (2011).
- [72] Antoine Georges, Luca de’ Medici, and Jernej Mravlje, “Strong correlations from Hund’s coupling,” *Annual Review of Condensed Matter Physics* **4**, 137–178 (2013).
- [73] Luca de’ Medici, “Hund’s metals, explained,” E. Pavarini, E. Koch, R. Scalettar, and R. Martin (eds.) *The Physics of Correlated Insulators, Metals, and Superconductors Modeling and Simulation Vol. 7* Forschungszentrum Juelich, 2017, ISBN 978-3-95806-224-5 (2017), [arXiv:1707.03282](https://arxiv.org/abs/1707.03282).
- [74] K.M. Stadler, G. Kotliar, A. Weichselbaum, and J. von Delft, “Hundness versus Mottness in a three-band HubbardHund model: On the origin of strong correlations in Hund metals,” *Annals of Physics* **405**, 365 – 409 (2019).
- [75] M. A. Hayward, M. A. Green, M. J. Rosseinsky, and J. Sloan, “Sodium hydride as a powerful reducing agent for topotactic oxide deintercalation: synthesis and characterization of the Nickel(I) Oxide LaNiO₂,” *Journal of the American Chemical Society* **121**, 8843–8854 (1999).
- [76] M.A. Hayward and M.J. Rosseinsky, “Synthesis of the infinite layer Ni(I) phase NdNiO_{2+x} by low temperature reduction of NdNiO₃ with sodium hydride,” *Solid State Sciences* **5**, 839 – 850 (2003), international Conference on Inorganic Materials 2002.
- [77] Shoji Ishibashi, Kiyoyuki Terakura, and Hideo Hosono, “A possible ground state and its electronic structure of a mother material (laofeas) of new superconductors,” *Journal of the Physical Society of Japan* **77**, 053709 (2008).
- [78] Q. Huang, Y. Qiu, Wei Bao, M. A. Green, J. W. Lynn, Y. C. Gasparovic, T. Wu, G. Wu, and X. H. Chen, “Neutron-diffraction measurements of magnetic order and a structural transition in the parent BaFe₂As₂ compound of FeAs-based high-temperature superconductors,” *Phys. Rev. Lett.* **101**, 257003 (2008).
- [79] Kenji Ishida, Yusuke Nakai, and Hideo Hosono, “To what extent iron-pnictide new superconductors have been clarified: A progress report,” *Journal of the Physical Society of Japan* **78**, 062001 (2009).

- [80] N. Qureshi, Y. Drees, J. Werner, S. Wurmehl, C. Hess, R. Klingeler, B. Büchner, M. T. Fernández-Díaz, and M. Braden, “Crystal and magnetic structure of the oxypnictide superconductor $\text{LaFeAsO}_{1-x}\text{F}_x$: A neutron-diffraction study,” *Phys. Rev. B* **82**, 184521 (2010).
- [81] S. V. Borisenko, V. B. Zabolotnyy, D. V. Evtushinsky, T. K. Kim, I. V. Morozov, A. N. Yaresko, A. A. Kordyuk, G. Behr, A. Vasiliev, R. Follath, and B. Büchner, “Superconductivity without nesting in LiFeAs ,” *Phys. Rev. Lett.* **105**, 067002 (2010).
- [82] P. Hansmann, R. Arita, A. Toschi, S. Sakai, G. Sangiovanni, and K. Held, “Dichotomy between large local and small ordered magnetic moments in iron-based superconductors,” *Phys. Rev. Lett.* **104**, 197002 (2010).
- [83] A. Toschi, R. Arita, P. Hansmann, G. Sangiovanni, and K. Held, “Quantum dynamical screening of the local magnetic moment in Fe-based superconductors,” *Phys. Rev. B* **86**, 064411 (2012).
- [84] Qiangqiang Gu, Yueying Li, Siyuan Wan, Huazhou Li, Wei Guo, Huan Yang, Qing Li, Xiyu Zhu, Xiaoqing Pan, Yuefeng Nie, and Hai-Hu Wen, “Two superconducting components with different symmetries in $\text{Nd}_{1-x}\text{Sr}_x\text{NiO}_2$ films,” (2020), [arXiv:2006.13123](https://arxiv.org/abs/2006.13123).
- [85] H. Miao, W. H. Brito, Z. P. Yin, R. D. Zhong, G. D. Gu, P. D. Johnson, M. P. M. Dean, S. Choi, G. Kotliar, W. Ku, X. C. Wang, C. Q. Jin, S.-F. Wu, T. Qian, and H. Ding, “Universal $2\Delta_{max}/k_B T_c$ scaling decoupled from the electronic coherence in iron-based superconductors,” *Phys. Rev. B* **98**, 020502 (2018).
- [86] Francesco Petocchi, Viktor Christiansson, Fredrik Nilsson, Ferdi Aryasetiawan, and Philipp Werner, “Normal state of $\text{Nd}_{1-x}\text{Sr}_x\text{NiO}_2$ from self-consistent $\text{GW}+\text{EDMFT}$,” (2020), [arXiv:2006.00394](https://arxiv.org/abs/2006.00394).
- [87] Koichi Momma and Fujio Izumi, “VESTA: a three-dimensional visualization system for electronic and structural analysis,” *Journal of Applied Crystallography* **41**, 653–658 (2008).
- [88] P. E. Blöchl, “Projector augmented-wave method,” *Phys. Rev. B* **50**, 17953–17979 (1994).
- [89] G. Kresse and D. Joubert, “From ultrasoft pseudopotentials to the projector augmented-wave method,” *Phys. Rev. B* **59**, 1758–1775 (1999).
- [90] John P. Perdew, Kieron Burke, and Matthias Ernzerhof, “Generalized gradient approximation made simple,” *Phys. Rev. Lett.* **77**, 3865–3868 (1996).

Supplementary Materials for “Hund’s metal physics: from SrNiO₂ to NdNiO₂”

Y. Wang,¹ C.-J. Kang,² H. Miao,³ and G. Kotliar^{1,2}

¹*Department of Condensed Matter Physics and Materials Science,
Brookhaven National Laboratory, Upton, New York 11973, USA*

²*Department of Physics and Astronomy, Rutgers University, Piscataway, New Jersey 08856, USA*

³*Material Science and Technology Division, Oak Ridge National Laboratory, Oak Ridge, Tennessee 37830, USA*
(Dated: June 30, 2020)

S-I. COMPUTATIONAL DETAILS

Fig. S1(a) shows the crystal structure of La(Sr)NiO₂ generated by the VESTA software¹. Fig. S1(b) shows the corresponding Brillouin zone (BZ) and the high-symmetry K -path used in the band structure plots. The spin-polarized calculations are performed on the static mean-field level using the DFT+ U method implemented in the VASP package² with projector augmented-wave (PAW) pseudopotential^{3,4} and Perdew-Burke-Ernzerhof parametrization of the generalized gradient approximation (GGA-PBE) exchange-correlation functionals⁵. The energy cutoff of the plane-wave basis is set to be 600 eV, and a Γ -centered $20 \times 20 \times 20$ K -point grid is used. Fig. S2 shows the magnetic configurations considered in the calculations.

S-II. FERMI SURFACE

Fig. S3 shows the DFT+DMFT Fermi surfaces (FSs) cuts at $k_z = 0, 0.0625, 0.125, 0.25, 0.375, 0.4375, 0.5$ for LaNiO₂ (upper panel) and SrNiO₂ (lower panel). The FSs of LaNiO₂ contain three sheets^{6,7}: (1) an electron-like pocket around Γ -point with mainly Ni- $d_{3z^2-r^2}$ and La- $5d$ characters; (2) another electron-like pocket around A -point with mainly Ni- $d_{xz/yz}$ and interstitial La- s characters; (3) a hole-like FS centered along the A - M BZ edge with Ni- $d_{x^2-y^2}$ character, which is just at the von Hove singularity point [see Fig. S3(g) at $k_z = 0.5$], indicating Lifshitz transition upon hole-doping. The FSs of SrNiO₂ also contain three sheets: (1) an electron-like FS around Γ -point with mainly Ni- $d_{x^2-y^2}$ character; (2) a hole-like FS centered along A - M BZ edge with mainly Ni- $d_{xz/yz}$ character; (3) another hole-like FS centered along A - M BZ edge with mainly Ni- $d_{xz/yz}$ and $-d_{3z^2-r^2}$ characters.

¹ Koichi Momma and Fujio Izumi, “Vesta: a three-dimensional visualization system for electronic and structural analysis,” *Journal of Applied Crystallography* **41**, 653–658 (2008).
² G. Kresse and J. Furthmüller, “Efficient iterative schemes for *ab initio* total-energy calculations using a plane-wave basis set,” *Phys. Rev. B* **54**, 11169–11186 (1996).
³ P. E. Blöchl, “Projector augmented-wave method,” *Phys. Rev. B* **50**, 17953–17979 (1994).
⁴ G. Kresse and D. Joubert, “From ultrasoft pseudopotentials to the projector augmented-wave method,” *Phys. Rev. B*

59, 1758–1775 (1999).

⁵ John P. Perdew, Kieron Burke, and Matthias Ernzerhof, “Generalized gradient approximation made simple,” *Phys. Rev. Lett.* **77**, 3865–3868 (1996).
⁶ I. Leonov, S. L. Skornyakov, and S. Y. Savrasov, “Lifshitz transition and frustration of magnetic moments in infinite-layer ndnio₂ upon hole-doping,” (2020), [arXiv:2003.04368](https://arxiv.org/abs/2003.04368).
⁷ Jonathan Karp, Antia S. Botana, Michael R. Norman, Hyowon Park, Manuel Zingl, and Andrew Millis, “Many-body electronic structure of ndnio₂ and cacuo₂,” (2020), [arXiv:2001.06441](https://arxiv.org/abs/2001.06441).

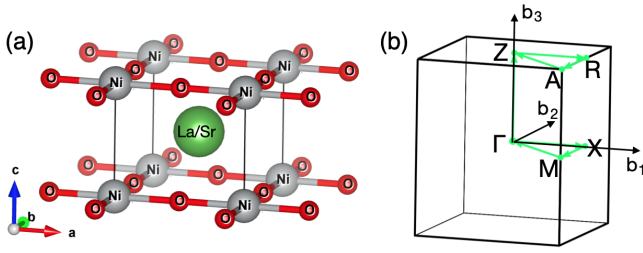


FIG. S1. (a) The crystal structure of LaNiO_2 or SrNiO_2 . (b) The Brillouin zone and high-symmetry K -path.

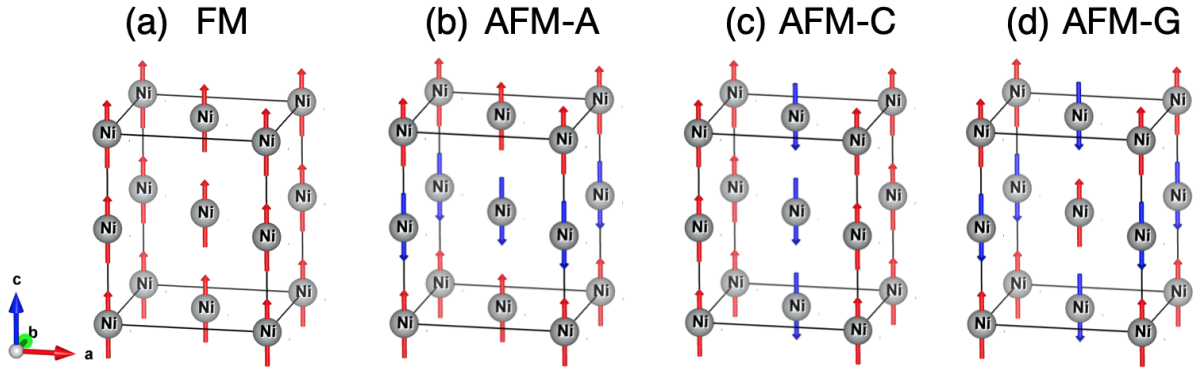


FIG. S2. Magnetic configurations with a $\sqrt{2} \times \sqrt{2} \times 2$ supercell. Arrows indicate spin directions on the Ni sites. (a) ferromagnetic (FM), (b) ferromagnetic in plane and antiferromagnetic out of plane (AFM-A), (c) antiferromagnetic in plane and ferromagnetic out of plane (AFM-C) and (d) antiferromagnetic in plane and antiferromagnetic out of plane (AFM-G).

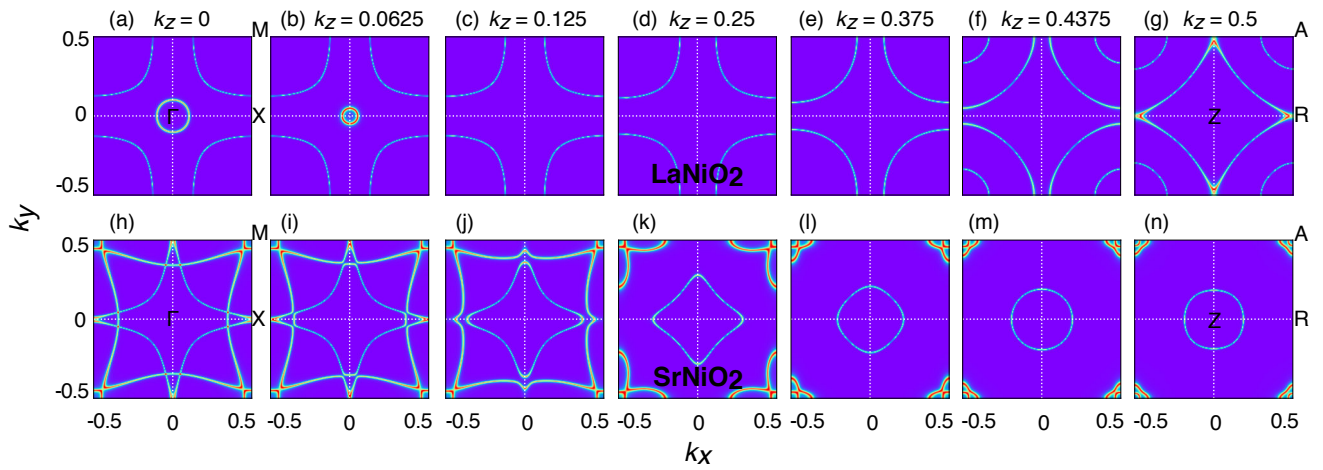


FIG. S3. The DFT+DMFT Fermi surfaces at $k_z = 0, 0.0625, 0.125, 0.25, 0.375, 0.4375, 0.5$. (a)-(g) for LaNiO_2 and (h)-(n) for SrNiO_2 .